Metal-insulator segregation in lithium rich Li n H m + clusters

R. Antoine, Ph. Dugourd, D. Rayane, E. Benichou, and M. Broyer

Citation: The Journal of Chemical Physics **107**, 2664 (1997); doi: 10.1063/1.474628
View online: http://dx.doi.org/10.1063/1.474628
View Table of Contents: http://scitation.aip.org/content/aip/journal/jcp/107/7?ver=pdfcov
Published by the AIP Publishing

Metal-insulator segregation in lithium rich $Li_nH_m^+$ clusters

R. Antoine, Ph. Dugourd, D. Rayane, E. Benichou, and M. Broyer
Laboratoire de Spectrométrie Ionique et Moléculaire (UMR no 5579), CNRS et Université Lyon I, bâtiment 205, 43 Bd du 11 Novembre 1918, 69622 Villeurbanne Cedex, France

(Received 18 March 1997; accepted 8 May 1997)

The metallicity of lithium rich $Li_nH_m^+$ cluster ions $[1 \leqslant m \leqslant 6,\ n \leqslant 22,$ and $(n-m) > 3]$ is studied by measuring unimolecular dissociation rates. These clusters are found to decompose by evaporation of a Li atom or a Li_2 molecule. The evaporative rates of mixed clusters display features characteristic of metallic clusters. This confirms and extends to a larger size range the previous results obtained by photoionization and absorption cross-section measurements. The simulation of the evaporative rates, with a statistical Rice–Ramsperger–Kassel (RRK) model which has been adapted to mixed clusters, confirms that there is a clear separation between a metallic Li_{n-m}^+ part and an insulating $(LiH)_m$ part. © *1997 American Institute of Physics.* [S0021-9606(97)02631-7]

I. INTRODUCTION

Metal–nonmetal transition in finite systems provides information on the fundamental issues of the metal–nonmetal transition in the solid as well as on interfacial problems. The metallisation of a small particle can occur by a smooth and gradual metallisation of the whole particle or by a separation of a metallic part and an insulating part in the particle. In the later case, problems similar to the metallic wetting of an insulating surface are encountered. Metallization of clusters have been studied in metal-oxide[1–4] (Cs–O, Li–O, Ba–O,...) and alkali halide clusters.[5–7] In alkali-oxide clusters, the metal atoms in excess may form a metallic layer around an insulating core, but metal-oxide are very complex systems. The lattice structures of the solid are complex and the study of the cesium oxidation shows that there may be competition between different suboxide or peroxide phases on the metal surface.[8] The structure of alkali halide clusters are well defined, they are totally ionic and have a cubic NaCl structure.[9–11] The ionic structure is very pronounced. In particular, in systems with a few electrons in excess, the localization of the electrons in excess is governed by the ionic structure.[10,12] In small NaCl and NaF clusters with sodium atoms in excess, a separation between a metallic part and a ionic part has been observed.[6] Lithium hydride has the same NaCl structure. Due to the low electronegativity of hydrogen, the ionic character is less pronounced than in alkali halides. Moreover, on the electronic point of view, this system is the simplest mixed system that can be built (1 electron for hydrogen atoms and 3 for lithium atoms). Lithium hydride clusters appear as a very simple system to study metallization problems. The approach is more general than in alkali halide clusters where the properties of the insulating part and of the interface are totally driven by the ionic interactions.[7]

In a recent paper,[13] we have reported results of unimolecular decay experiments for the quasi-stoichiometric $(LiH)_nLi^+$ and $(LiH)_nLi_3^+$ clusters. A total loss of the metallic character is observed for both cluster series. They seem to have cubic lattice structures similar to the structure of the bulk. A significant change in the electronic properties is observed when the proportion of metal atoms increases in the clusters. Some previous results have been obtained by absorption cross-section measurements of Li_nH clusters[14] and by photoionization measurements of the sparsely hydrogenated Li_nH_m clusters.[15,16] These results show that for a small number of hydrogen atoms, a lithium electron is localized by each H atom and the other $(n-m)$ electrons remain delocalized. This interpretation is confirmed by *ab initio* calculations and structures have been determined for small sizes. The geometric structures of Li_nH_2 and Li_nH_3 determined by Koutecky *et al.*[17] show that the hydrogen atoms do not penetrate in the cluster, but instead they stick on the surface, with a tendency to become localized on one side of the cluster. For clusters with only two lithium atoms in excess, the calculated structures point out a separation between a metallic part and an insulating part.[18] The experimental studies have been limited to small and sparsely hydrogenated clusters and theoretical studies to very small sizes.

In this article, we study Li_nH_m clusters with up to six hydrogen atoms in order to investigate the evolution from the sparsely hydrogenated clusters, which display metallic features, to the $(LiH)_nLi_3^+$ and $(LiH)_nLi^+$ clusters, which display nonmetal features. Absorption cross sections and photoionization efficiencies are long and difficult data to obtain. To be able to study a wide range of sizes we measured the unimolecular evaporative rates of $Li_nH_m^+$ clusters $(1 \leqslant m \leqslant 6,\ n \leqslant 22)$. All the clusters studied in this experiment with $n-m > 3$ display metallic features. Simulations of the evaporative rates with a Rice–Ramsperger–Kassel (RRK) statistical model show that there is a clear separation between an insulating part and a metallic part.

II. EXPERIMENT

A detailed description of the experimental setup was published previously,[13] and only a brief outline is given here. The neutral lithium Li_n and hydrogenated lithium Li_nH_m clusters are produced in a seeded molecular beam. Isotopically pure lithium ^7Li is heated up to 1200 °C in a titanium zirconium molybdenum alloy oven. The lithium vapor (about 100 Torr) is expanded through a 100 μm nozzle with 3 or 4

 0021-9606/97/107(7)/2664/9/$10.00

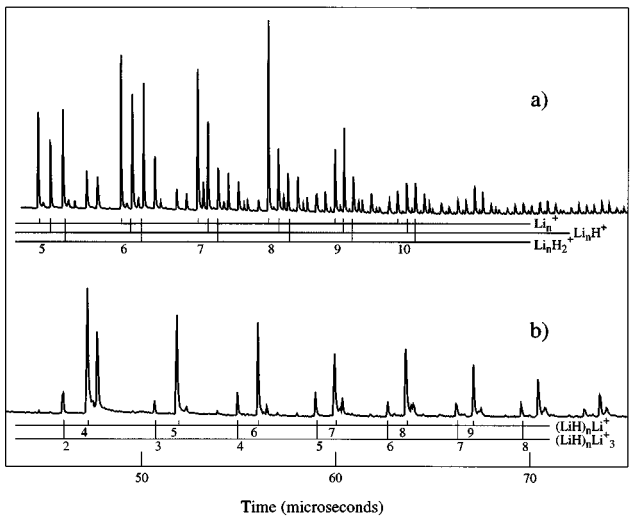

FIG. 1. Mass spectra of hydrogenated lithium clusters ionized with different laser conditions: (a) $h\nu = 4.96$ eV and $\Phi = 1$ mJ/cm^2. (b) $h\nu = 3.49$ eV and $\Phi = 300$ mJ/cm^2.

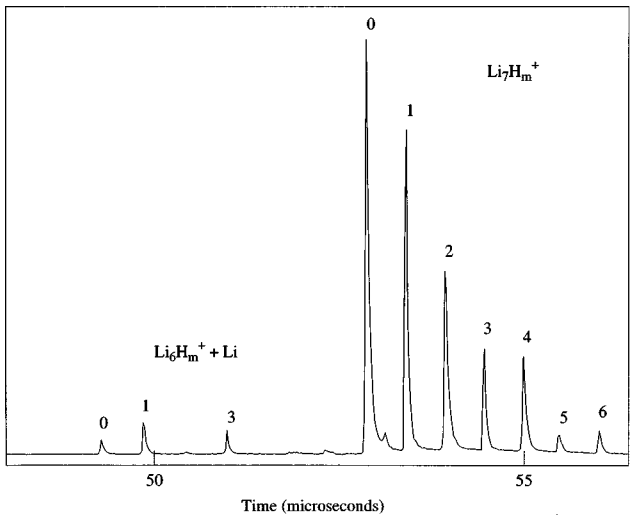

FIG. 2. Mass spectrum of $Li_7H_m^+$ clusters and their fragments.

bars of argon mixed with 4% of hydrogen. The clusters are ionized by a XeCl pumped tunable dye laser. The energy of the laser, after frequency doubling in a BBO crystal ($h\nu = 4.6-5.5$ eV) allows for a direct photoionization of the clusters. The ions are mass-analyzed with a reflectron time-of-flight mass spectrometer. They are extracted and accelerated by 900 V. They fly a first $\cong 1$ m long electrical field free region (time window $[t1,t2]$). Then, they are reflected by an electrostatic mirror and they travel through a second field free region toward a detector (microchannel plates). The reflectron allows us to observe the unimolecular decay which occurs during the first time of flight $[t1,t2]$. If a metastable parent ion evaporates during this time, the resulting daughter ion has a shorter reflective travel in the reflectron than the corresponding parent ion (due to its smaller kinetic energy). After the second field free region, the parent and daughter ions are collected at different times. By applying a suitable electrical pulse to the deflective plates of a mass gate located in the first time of flight, a single mass packet and its corresponding fragments can be detected. With our experimental device, the time of extraction is $t_1 \cong 0.3\sqrt{n+(m/7)}\ \mu$s and the duration of the first flight is $t_2 - t_1 \cong 8.0\sqrt{n+(m/7)}\ \mu$s for the $Li_nH_m^+$ cluster.

III. EXPERIMENTAL RESULTS

A. Mass spectra of hydrogenated lithium clusters

Figure 1 displays two mass spectra of hydrogenated lithium clusters recorded for different conditions of ionization. The voltages of the horizontal deviation plates in the ionization source were set to maximize the signal for cluster sizes with 10–20 lithium atoms. The same sets of parameters and the same source conditions were used for both spectra. Figure 1(a) shows a mass spectrum of clusters ionized by a UV laser ($h\nu = 4.96$ eV) at low laser fluence (1 mJ/cm^2). The energy of the photon is higher than the ionization potentials of the clusters, the laser fluence is low. The clusters are ionized by a one-photon process and this spectrum is close to the distribution of the neutral clusters which are produced in the source. To the right of each pure lithium cluster peak, we observe the peaks due to the hydrogenated lithium clusters: Li_nH^+, $Li_nH_2^+$, etc. The very small peaks (for example, between Li_6^+ and Li_6H^+) are due to clusters which have evaporated during the first time of flight (cf. Fig. 2). The pure lithium clusters and the lithium rich mixed clusters are the most intense. The atomic mass of lithium is 7, $Li_nH_7^+$ and Li_{n+1}^+ overlap in the mass spectrum. However, with the low percentage of hydrogen (4%) used in the carrier gas for this experiment, the intensity of $Li_nH_m^+$ clusters decreases regularly with m, and becomes negligible for $Li_nH_7^+$. Figure 1(b) shows a mass spectrum of clusters ionized by the third harmonic of a Nd:YAG laser ($h\nu = 3.49$ eV) at very high laser power (300 mJ/cm^2). In the spectrum 1(b), the lithium clusters have totally disappeared and only the mixed $(LiH)_nLi_m^+$ (with $m = 0$, 1, and 3) clusters are observed. Both spectra in Fig. 1 are radically different. In the spectrum 1(b), the photon energy ($h\nu = 3.49$ eV) is below the ionization potentials of small lithium and sparsely hydrogenated lithium clusters.[16] For such high laser fluence, multiphoton processes are extremely significant. For example, a pure lithium cluster with around 20 atoms may absorb up to 30 photons during the laser pulse.[19] Clusters are strongly heated, implying rapid evaporations and only the most stable ionic clusters are observed. The metal rich mixed clusters produced by the source [spectrum 1(a)] loose their lithium atoms in excess by rapid sequential evaporations, leading to the quasi-stoichiometric lithium hydride clusters [spectrum 1(b)]. The clusters observed in this spectrum are particularly stable. The sequential evaporation of metal atoms is confirmed by our study of the unimolecular evaporation of lithium rich $Li_nH_m^+$ clusters.

We used the mass gate to measure the evaporative rates. We systematically recorded the mass packets corresponding to Li_n^+ and its hydrides $Li_nH_m^+$. Figure 2 shows an example of unimolecular evaporation spectrum for $Li_7H_m^+$ ($0 \leqslant m$

$\leqslant 6$) clusters. The main peaks on the right correspond to the $Li_7H_m^+$ parent ions. On the left of the spectrum, we observe the peaks of the fragments resulting from the unimolecular decay of $Li_7H_m^+$ clusters. The fragment peaks are due to the evaporation of one lithium atom. Evaporation is observed only for mixed clusters with an odd number of valence electrons $(n-m-1)$. These clusters are less stable than the clusters with an even number of valence electrons.

B. Unimolecular evaporation results

To measure the evaporative rates we ionized the clusters with a UV laser ($h\nu = 4.96$ eV) and a low laser power ($1\ \mathrm{mJ/cm^2}$). All the possible unimolecular decay channels were examined for the lithium rich $Li_nH_m^+$ clusters ($0 \leqslant m \leqslant 6$ and $n \leqslant 22$). For the $Li_nH_m^+$ clusters with $(n-m) > 3$, only two channels of evaporation have been observed. The evaporative channels correspond to the loss of a Li atom (monomer) or a Li_2 molecule (dimer). The same channels are observed for the pure lithium clusters.

$$Li_nH_m^+ \rightarrow Li_{n-1}H_m^+ + Li \quad (a)$$

$$Li_nH_m^+ \rightarrow Li_{n-2}H_m^+ + Li_2 \quad (b)$$

Different channels of evaporation were observed for the quasi-stoichiometric lithium hydride clusters.[13] When they are ionized with a high laser fluence [Fig. 1(b)], $Li_nH_m^+$ (or $(LiH)_mLi_{n-m}^+$) clusters with $(n-m) = 0, 1, 3$ evaporate LiH and Li_2H_2 molecules. Some of these clusters are observed in the mass spectrum of Fig. 1(a), but they do not evaporate with the present ionization conditions. In both experiments, these clusters are in an evaporative ensemble but with different temperatures.[2] In the present experiment, the temperature of the clusters is fixed by the binding energies of the metallic part (cf. next section), while at high laser power the temperature is fixed by the binding energies of the insulating part. The temperature is higher in the second case. So quasi-stoichiometric clusters and lithium rich clusters have different decay channels. The dissociative energies are higher for the quasi-stoichiometric clusters.

For each $Li_nH_m^+$ cluster, the total fractional dissociation rate F_n is

$$F_n = \frac{I_{n-2,m} + I_{n-1,m}}{I_{n-2,m} + I_{n-1,m} + I_{n,m}}, \quad (1)$$

where $I_{n,m}$, $I_{n-1,m}$ and $I_{n-2,m}$ are the peak intensities of the remaining $Li_nH_m^+$ parent ion and of the ionic fragments, respectively. In order to probe the competition between the two pathways of dissociation, we define the branching ratio for the loss of a monomer as

$$Br_1 = \frac{I_{n-1,m}}{I_{n-2,m} + I_{n-1,m}}. \quad (2)$$

For each size, we measured the total evaporative rate F_n and the branching ratio Br_1 of $Li_nH_m^+$ clusters. We estimated the experimental reproducibility equal to 5% for the total evaporative rates, and 10% for the branching ratios.

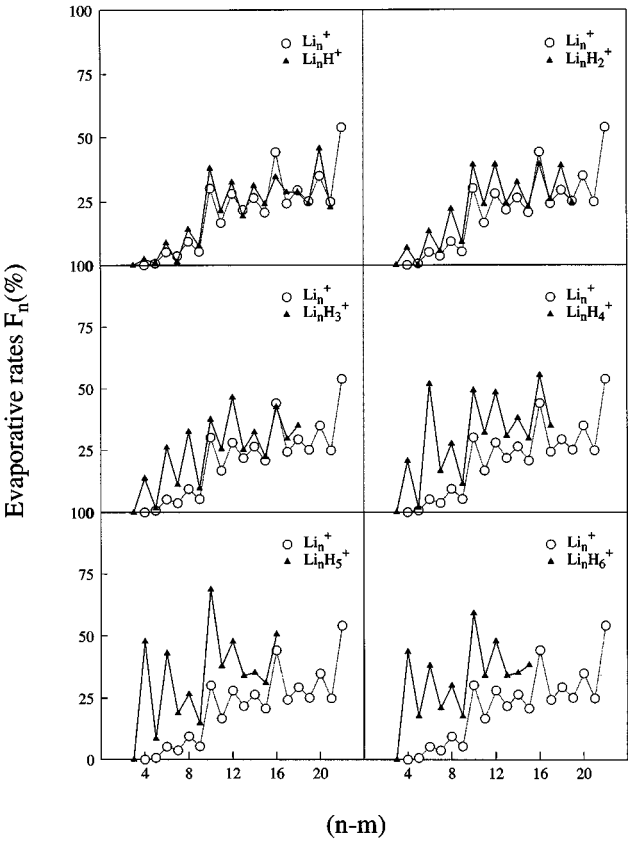

FIG. 3. Experimental evaporative rates F_n of $Li_nH_m^+$ and Li_n^+ clusters plotted as a function of $(n-m)$.

The comparison between the ionization potentials of Li_nH_m clusters and the ionization potentials of the bare lithium Li_n clusters[15,16] led to the conclusion that the electronic properties of Li_nH_m clusters were driven by the number of free valence electrons $(n-m)$. As for the ionization potential analysis, we compare the evolution of the evaporative rates of mixed clusters in respect to the number of free electrons. We have plotted in Fig. 3 the evolution of the total evaporative rates F_n for the $Li_nH_m^+$ clusters as a function of $(n-m)$. These rates are compared to the evaporative rates of pure lithium clusters. The evaporation of bare lithium clusters have been studied by Bréchignac *et al.*[20] Although our conditions of ionization are very different, we obtained very similar values for the total evaporative rates. The total evaporative rates of lithium clusters are characterized by a general increase with the cluster size. An odd–even alternation is superimposed on this global increase; odd-sized clusters (even number of electrons) are more stable (lower evaporative rates) than the even sizes (odd number of electrons). Some clusters have particularly low decay rates in respect to the other sizes, they are very stable versus the evaporation process. In this size range, the low decay rate of Li_9^+ is characteristic of the $1p$ shell closing (eight electrons). Figure 3 shows that the $Li_nH_m^+$ clusters have the same behavior concerning the evaporation process as the

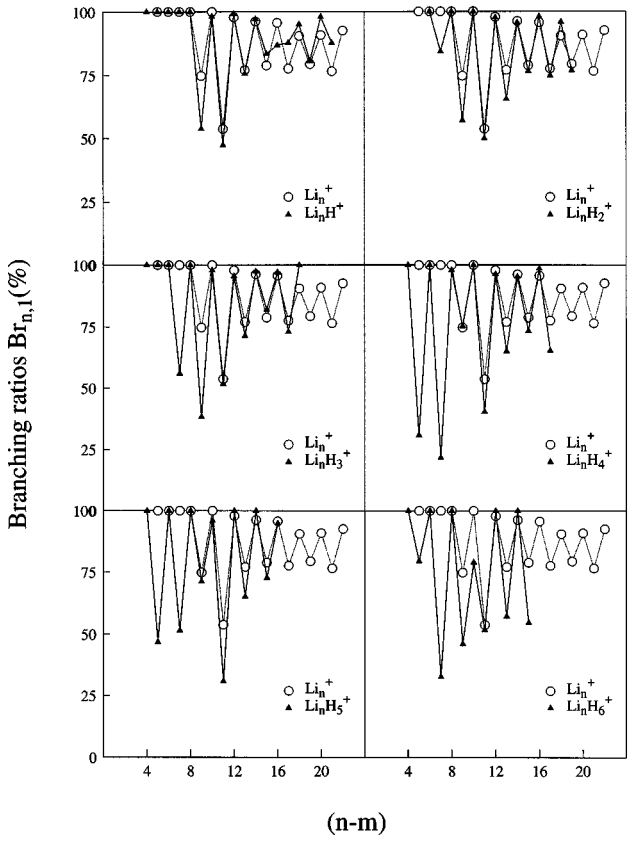

FIG. 4. Experimental branching ratios of $Li_nH_m^+$ and Li_n^+ clusters corresponding to the loss of a Li atom (Br_1).

Li_{n-m}^+ clusters. The odd–even alternation and the decrease between $Li_{9+m}H_m^+$ and $Li_{10+m}H_m^+$ clusters are still observed in the total dissociation rates of metal rich $Li_nH_m^+$ clusters. Even the details of the evaporative rates for the mixed clusters are analogous to the details for the corresponding lithium clusters. For example, low rates are observed for $Li_{15+m}H_m^+$ clusters and high rates for $Li_{16+m}H_m^+$ clusters. Finally, we note a regular increase of the evaporative rates with the number of hydrogen atoms in the mixed clusters. We see in Fig. 3 that the rates of $Li_nH_4^+$, $Li_nH_5^+$, and $Li_nH_6^+$ clusters are globally higher (but with the same behavior) than the bare lithium cluster rates. We will show in the next section that this increase in the evaporative rates is due to an increase in the number of vibrational modes in the mixed clusters.

In the same way, we have plotted in Fig. 4, the branching ratios for the loss of a monomer Br_1 for the $Li_nH_m^+$ clusters as a function of $(n-m)$. These ratios are also compared to the branching ratios of the pure lithium clusters. Lithium clusters with an even number of atoms evaporate principally monomers of lithium ($Br_1 \sim 100\%$), whereas the clusters with an odd number of atoms evaporate monomers and dimers ($Br_1 < 100\%$). This is due to the higher stability of metal clusters with an even number of free electrons. The odd–even alternation amplitude decreases as cluster size increases. Once again, the odd–even alternation and the decrease in its amplitude with the cluster size are still observed for the lithium rich $Li_nH_m^+$ cluster branching ratios. Except for the smallest sizes, the monomer–dimer competition does not seem to be affected by the hydrogen atoms. For the smallest sizes, the clusters with an odd $n-m$ value (even number of electrons) tend to evaporate both dimers and monomers while pure lithium clusters evaporate monomers. This tendency to evaporate dimers increases as m increases.

IV. DISCUSSION

Our results on unimolecular evaporation experiments for the lithium rich $Li_nH_m^+$ clusters confirm, and extend to a larger size range, the previous results obtained with the photoionization and absorption cross-section measurements. The main characteristics (i.e., odd–even alternation, shell effects, and monomer–dimer competition) and even the details of the evaporative rates of metallic clusters are well reproduced in the mixed clusters. In a first approximation, the $Li_nH_m^+$ clusters have the electronic properties of the metallic Li_{n-m}^+ clusters with $(n-m-1)$ free valence electrons. Every H atom localizes one lithium valence electron the other valence electrons remain delocalized. The observation of electronic shell closing is particularly worth notice. The free electron cloud remains globally spherical in the $Li_nH_m^+$ clusters (at least for clusters with a large number of lithium atoms in excess). We also want to emphasize that a change of 0.05 eV in the dissociation energies may result in a change of 10% in the evaporative rates and may have dramatic consequences in the branching ratios. Thus the Li_{n-m}^+ part is not substantially perturbed by the other atoms. Only a clear separation between a metallic part and an insulating part, where the dynamics of evaporation would be governed by the binding energies of the metallic part, seems to be able to explain these results. To test this assumption we have modeled the evaporation of $Li_nH_m^+$ clusters.

A. Model for the evaporation of $Li_nH_m^+$ clusters

To simplify the reading of this section, the details of the calculation and the formula are given in appendixes. The crude statistical model that we use to study the evaporation process is based on two assumptions: (i) There is a segregation in the mixed cluster between a metallic part and an insulating part. (ii) The binding energies of $Li_nH_m^+$ clusters are equal to the binding energies of Li_{n-m}^+. The $(LiH)_m$ insulating part acts as a reservoir of energy (internal vibrational modes) for the mixed cluster. To calculate the dissociation rates, we used a statistical RRK model[21] that we have adapted to the evaporation of mixed clusters.[13] The calculation of the evaporative rate as a function of the internal energy for a mixed cluster is described in Appendix A.

To simulate the evaporative rates of the lithium rich $Li_nH_m^+$ clusters, we assume that they form an evaporative ensemble.[22] In an evaporative ensemble, a cluster dissipates its internal energy only by evaporation and has undergone at least one evaporation. The mixed $Li_nH_m^+$ clusters are ionized at low laser fluence with a photon energy higher than their ionization potentials. There is some energy in excess during the photoionization. We have shown that a part of this

TABLE I. Dissociation energies $D^+_{n,1}$ and $D^+_{n,2}$ of Li_n^+ clusters corresponding to the evaporation of a monomer and of a dimer.

n	$D^+_{n,1}$ (eV)[a]	$D^+_{n,2}$ (eV)[a]
4	0.80	1.24
5	1.66	1.40
6	1.20	1.80
7	1.34	1.48
8	1.03	1.31
9	1.60	1.57
10	0.83	1.37
11	1.30	1.07
12	1.04	1.28
13	1.20	1.18
14	1.09	1.23
15	1.23	1.26
16	1.08	1.25
17	1.22	1.24
18	1.14	1.30
19	1.31	1.39
20	1.16	1.41
21	1.35	1.45
22	1.04	1.33
23	1.21	1.19
24	1.11	1.26
25	1.20	1.25

[a]C. Bréchignac, H. Busch, Ph. Cahuzac, and J. Leygnier, J. Chem. Phys. **101**, 6992 (1994).

energy in excess is transferred to the internal vibrational modes of the clusters.[23] Our beam produces hot neutral clusters, a small increase in energy is enough to prompt evaporations during the extraction time. The experimental evaporative rates that we measured for the bare lithium clusters are similar to those obtained by Bréchignac *et al.* at very high laser fluence. Moreover, our rates do not depend on the laser energy but only on the experimental time parameters t_1 and t_2, which is expected in an evaporative ensemble. Even if we are not in a perfect evaporative ensemble, we are close to it. In the frame of the evaporative ensemble, we have resolved the rate equations for the formation of the $Li_nH_m^+$ cluster packet at t_1 (considering that they are formed either by a monomer Li or by a dimer Li_2 evaporation) and for its evaporation during the first flight $[t_1,t_2]$. The formula for the total evaporative rates and for the branching ratios are given in Appendix B.

B. Simulation and discussion of the evaporative rates

We have simulated the total evaporative rates F_n and the branching ratios for the loss of a monomer Br_1 of the lithium rich $Li_nH_m^+$ clusters using the expressions (B1) and (B2). As already mentioned, we used the dissociation energies of Ref. 20 determined for the bare lithium clusters. These binding energies are listed in the Table I. The results of the simulation are plotted in Fig. 5. In order to show the effect of the metallic and insulating parts in the lithium rich $Li_nH_m^+$ clusters, we have plotted the simulated and experimental evaporative rates of the $(LiH)_mLi_{n-m}^+$ clusters, versus the number of (LiH) added. As already observed in Fig. 3, the experimental evaporative rates increase as the number of (LiH)

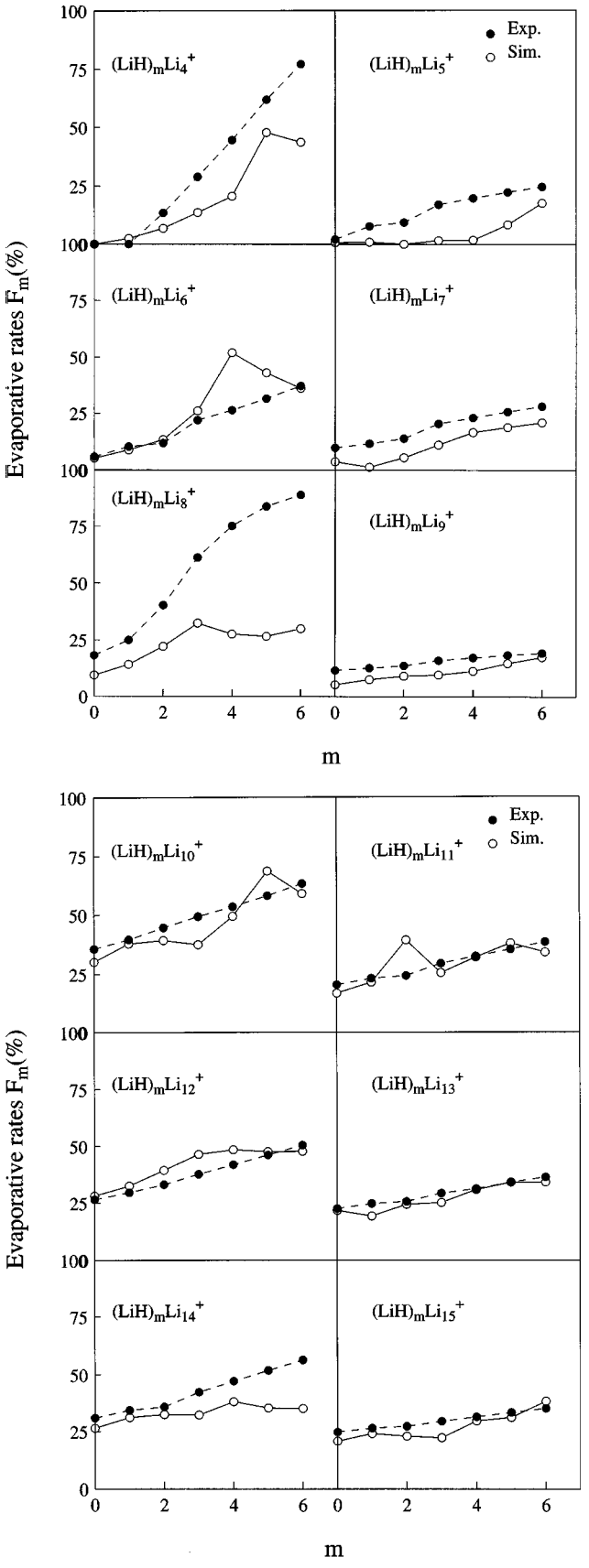

FIG. 5. (a) Experimental and simulated evaporative rates of $(LiH)_mLi_n^+$ clusters plotted as a function of the number of (LiH) units. (b) Experimental and simulated evaporative rates of $(LiH)_nLi_n^+$ clusters plotted as a function of the number of (LiH) units.

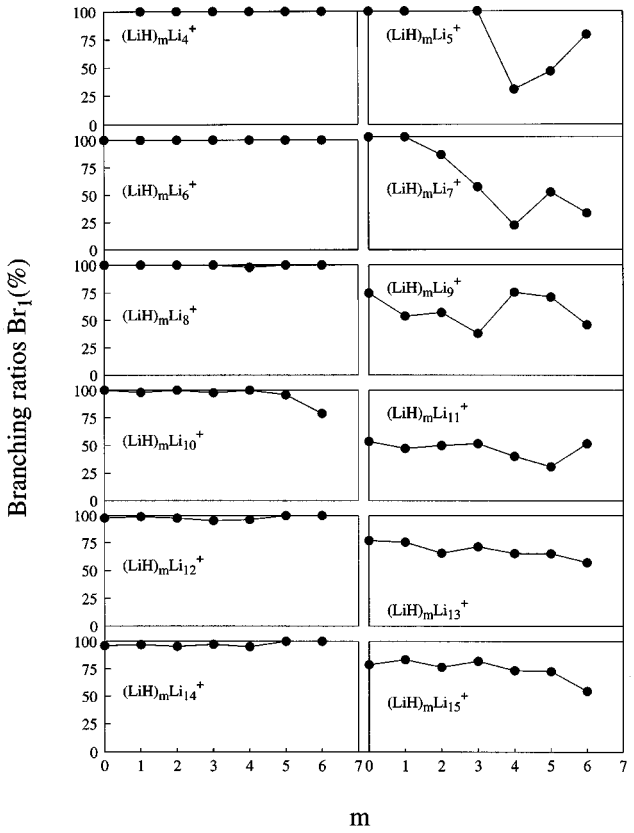

FIG. 6. Experimental branching ratio of $(LiH)_mLi_n^+$ clusters plotted as a function of the number m of (LiH) units.

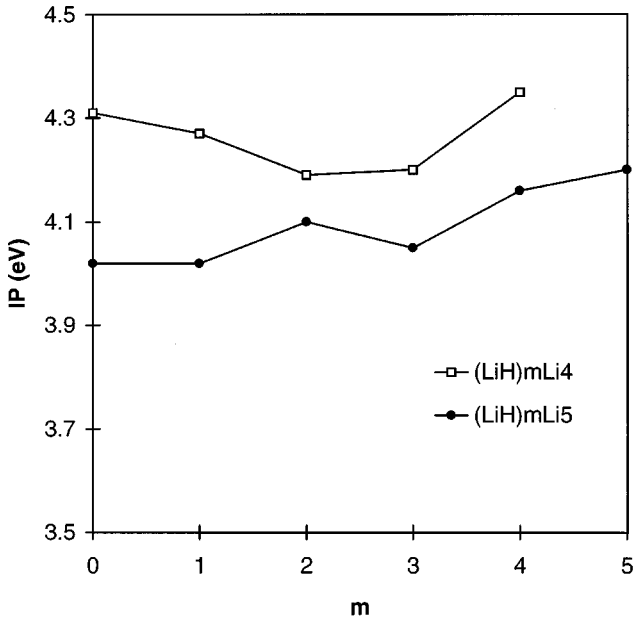

FIG. 7. Ionization potentials of $(LiH)_mLi_4$ clusters and $(LiH)_mLi_5$ clusters.

units increases. This increase is regular. This increase is more pronounced for small sizes than for large sizes and it is particularly steady for $n=4$, $n=6$, and $n=8$. The simulated rates also increase as the number of LiH units increases.

We discuss the clusters with $n-m>8$ first. Clusters with a small metallic part are discussed in the next paragraphs. For clusters with $n-m>8$, the simulated rates are in excellent agreement with the total experimental rates. This model is able to reproduce the little slop observed for $(LiH)_mLi_9^+$ as well as the steady slopes observed for $(LiH)_mLi_{10}^+$ or $(LiH)_mLi_{12}^+$. The increase in the evaporative rates is mainly due to the increase in the number of degrees of freedom in the cluster and not to a change in the binding energies. Figure 6 displays the experimental branching ratios corresponding to the loss of a monomer, as a function of the number of LiH units. For clusters with $n-m>8$, the branching ratios are almost constant as the number of LiH units increases. The branching ratios simulated with our model do not depend on the number of LiH units. Branching ratios are highly sensitive to the structure of the cluster, for example, the branching ratio measured on Li_{11}^+ depends on the formation process.[24] However, as expected in the frame of our crude model, we observe that for clusters with a large metallic core the insulating part does not induce any significant change in the branching ratios. For these clusters, the $(LiH)_m$ part is equivalent to a reservoir of energy and the interaction between the insulating part and the metallic part is weak.

For clusters with a small metallic part $(3<n-m<9)$, differences between simulations and experimental results are observed in Fig. 5(a) but the main trends are reproduced. The fact that details are not reproduced is not surprising. As the size of the metallic part decreases, the influence of the insulating part increases and the binding energies are certainly affected. Moreover, the precision in the determination of the binding energies of small lithium clusters is worse than in the large sizes, and statistical model may not be very reliable for very small sizes. Changes in the branching ratio are also observed whereas our model does not predict any change. Figure 6 shows that the branching ratios for $(LiH)_mLi_5^+$ and $(LiH)_mLi_7^+$ are strongly affected by the number of LiH units. The experimental ratios evolve rapidly from the monomer channel to the dimer channel. In contrary, for clusters with four, six, and eight atoms in excess only evaporation of monomer is observed whatever the number of LiH units. The changes in branching ratio for $(LiH)_mLi_5^+$ and $(LiH)_mLi_7^+$ are the most striking effect which are observed due to the increase of the insulating part. We believe that these changes are not due to the loss of a clearly segregated metallic part in the cluster. Indeed, Fig. 7 shows the ionization potentials measured on $(LiH)_mLi_4$ and $(LiH)_mLi_5$ clusters.[16] The ionization potentials are not too much affected by the insulating part. As already mentioned, these experimental values are in excellent agreement with values of *ab initio* calculations for structure with the hydrogen concentrated on one side of the cluster.[18] The stability of the ionization potentials shows that there are delocalized electrons in the mixed cluster and the adding of LiH units does not induce a strong modification in the electronic properties of the metallic part.

The change in evaporative pathway may result from a change in the surface energy of the metallic part due to its contact with the nonmetallic part. The cohesive energy of a neutral spherical metal cluster with n atoms can be modeled by the addition of a volume term and a surface term:

$$Ec(n)=na_v-\gamma S_o(n)=na_v-n^{2/3}a_s, \tag{3}$$

where a_v is the cohesive energy per atom, $S_o(n)$ is the surface of the cluster, and γ is the surface energy. Experimental values for lithium clusters are $a_v=1.52$ eV and $a_s=1.3$ eV.[20] An increase in the value of a_s induces an increase in the dimer channel. The increase in the surface $S(n)$ of the metal part, due to its laying on the nonmetal part (wetting of the nonmetal part by the metal part), is enough to explain the change in dissociative pathways. For the simulation below, we have chosen a surface increase of 50%: $S=(1+r)S_o$ with $r=0.5$. We suppose that the surface of contact S_c between the two parts depends only on the number of LiH units. S_c would correspond to the surface of one face of the insulating part. The cohesive energy can then be written as

$$Ec(n)=na_v-\gamma(S(n)-S_c)-\gamma_i S_c, \tag{4}$$

where γ_i can be assimilated to an interface energy. This formula supposes that the metallic part is not too diluted and that the interaction with the insulating part is not too strong. A metallic layer around an insulating part (or the reverse) would lead to totally different energies. The difference in cohesive energy between the free spherical metal cluster and the metallic part in the mixed cluster is obtained by subtraction of Eqs. (3) and (4):

$$\begin{aligned}\Delta Ec(n)&=\gamma(S_o(n)-S(n)+S_c)-\gamma_i S_c\\&=-r\gamma S_o(n)+(\gamma-\gamma_i)S_c.\end{aligned} \tag{5}$$

The difference in the binding energy of a monomer is then simply given by

$$\begin{aligned}\Delta D_{n,1}&=\Delta Ec(n)-\Delta Ec(n-1)\\&=-r\gamma(S_o(n)-S_o(n-1))\\&=-ra_s(n^{2/3}-(n-1)^{2/3})\end{aligned} \tag{6}$$

in the same way

$$\Delta D_{n,2}=-ra_s(n^{2/3}-(n-2)^{2/3}). \tag{7}$$

Differences in the binding energies for the ions are identical (providing that the ionization potentials are not modified). Dissociative energies for mixed clusters can be determined (in the frame of this model) by using Eqs. (6) and (7) and the dissociative energies of pure lithium clusters. We have plotted in Fig. 8 the differences $D^+_{n,2}-D^+_{n,1}$ for the pure lithium cluster and for a mixed cluster with a surface increase of 50%. This figure shows that the surface augmentation of the metallic part induces a decrease in the binding energy of the dimer as compared to the binding energy of the monomer. With $r=0.5$, clusters with an odd number of atoms would preferentially evaporate dimers, as it is observed for mixed clusters with a large (LiH) part. The evaluation of the exact shape of the metallic part is difficult and should be done for each cluster, a quantitative comparison was not possible. However, this model shows that an increase in the surface of the metallic part due to its laying on one face of the nonmetal part is enough to explain the change in the dissociative pathways.

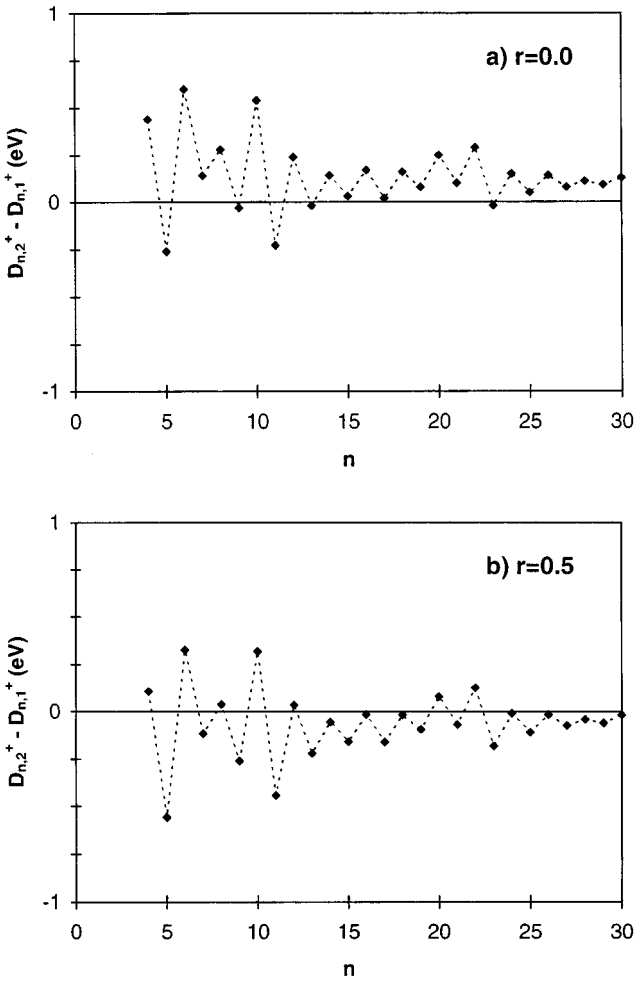

FIG. 8. Dimer binding energy minus monomer binding energy ($D^+_{n,2}-D^+_{n,1}$). (a) For pure lithium clusters. (b) For lithium clusters laying on an insulating part ($r=1.5$). See text for details.

Finally we want to emphasize again that for clusters with only 3 or 1 lithium atoms in excess, no evaporation of Li or Li_2 has been observed. However, for $Li_6H_3^+$, $Li_7H_4^+$, $Li_8H_5^+$, and $Li_9H_6^+$, our simple model [Eq. (B1)] with the dissociative energy of Li_3^+ (1.43 eV) predicts evaporative rates greater than 15%. The fact that these clusters do not evaporate is in contradiction with the results of our model of segregation. In fact only the evaporation of LiH units has been observed for these clusters (dissociative energy for the evaporation of LiH is around 2 eV and no evaporation is expected here[13]). The change in the evaporative pathway and in the stability is sudden, competition between LiH evaporation and Li or Li_2 evaporation is never observed. These changes seem to underline the loss of delocalized electrons in the cluster.

V. CONCLUSION

The unimolecular evaporation of $Li_nH_m^+$ clusters ($1\leqslant m\leqslant 6$) shows that clusters with as few as four lithium atoms in excess display metallic properties. As previously observed for small sizes, each H atom localizes one valence electron, the other electrons remain delocalized. The metallic

part is very little affected by the insulating part. As suggested by *ab initio* calculations on small sizes, there is a clear separation between the insulating part and the metallic part. An effect on the binding energies, due to the insulating part increase, has been observed only for clusters with a very small metallic part (less than seven lithium atoms in excess). Evaporation of dimers increases when the insulating part grows. This may be explained by a laying of the metallic part on the insulating part. No precursor of the sudden transition from metallic clusters to insulating clusters is observed.

APPENDIX A

We consider that in the $Li_nH_m^+$ clusters, the internal energy is randomly distributed among two kinds of oscillators with two different vibrational frequencies which correspond to the frequencies of the ground state of Li_2 ($\nu = 10.5\times10^{12}$ Hz) and LiH molecules ($\nu = 42.1 \times 10^{12}$ Hz).[25] The number of ways of arranging the internal energy E among the $s = s_{LiLi} + s_{LiH}$ internal modes is given by

$$\omega(E,s) = \sum_{p=0}^{p=E/h\nu_{LiH}} \omega((E - ph\nu_{LiH}), s_{LiH}) \times \omega'(ph\nu_{LiH}, s_{LiLi}), \tag{A1}$$

where $\omega((E-ph\nu_{LiH}),s_{LiH})$ and $\omega'(ph\nu_{LiH},s_{LiLi})$ are the numbers of ways of distributing the internal energy among the s_{LiH} oscillators and s_{LiLi} oscillators.[26] The probabilities of monomer evaporation $p_{n,1}(E,D_{n,1}^+)$ and of dimer evaporation $p_{n,2}(E,D_{n,2}^+)$ will be given by the probabilities of localizing enough internal energy (equal to the binding energies $D_{n,1}^+$ and $D_{n,2}^+$, respectively) in a single Li-Li mode:

$$p_{n,i}(E,D_{n,i}^+) = \frac{\sum_{p=0}^{p=(E-D_{n,i}^+)/h\nu_{LiH}} \omega((E-D_{n,i}^+ - ph\nu_{LiH}), s_{LiH})\,\omega'(ph\nu_{LiH}, s_{LiLi})}{\sum_{p=0}^{p=E/h\nu_{LiH}} \omega((E-ph\nu_{LiH}), s_{LiH})\,\omega'(ph\nu_{LiH}, s_{LiLi})} \quad (i=1,2). \tag{A2}$$

Then the partial rates $k_{n,i}(E)$ of dissociation will be

$$k_{n,i}(E) = g_i \nu_{LiH} p_n(E, D_{n,i}^+) \quad (i=1,2) \tag{A3}$$

and the total rate of dissociation

$$k_n(E) = k_{n,1}(E) + k_{n,2}(E). \tag{A4}$$

The frequency of energy redistribution in the cluster is given by the highest vibrational frequency ν_{LiH}. g_i corresponds to the degeneracy factor equal to the number of surface units capable of evaporating.[27] The degeneracy factor g_1 for the evaporation of a monomer is calculated by considering that all the outer atoms (n_{ext}) have the same probability of being evaporated, although the clusters are not exactly spherical. In the assumption of a metal-insulator segregation, since the insulating $(LiH)_m$ part does not evaporate, the number of surface units capable of evaporating is close to the number of atoms in the metallic Li_{n-m} part:

$$g_1 = n - m. \tag{A5}$$

For the degeneracy factor g_2 of dimer evaporation, by analogy with the earlier alkali works,[20,28] we took

$$g_2 = n - m - 1. \tag{A6}$$

Whereas the degeneracy factor g_1 is quite well justified, the proposed and applied value for g_2 is more problematic. Indeed, the most likely mechanism for the dimer evaporation is the evaporation of a dimer built from two outer neighboring atoms, then the degeneracy factor g_2 would be defined as

$$g_2 = \frac{\overline{\alpha}}{2}(n-m) = 3(n-m), \tag{A7}$$

where $\overline{\alpha}$ is the average number of surface coordination (theoretical works on alkali structures by Poteau and Spiegelmann[29] have shown that in the size range 10–20 atoms, $\overline{\alpha} \leqslant 6$). Our simulations show that a change in the degeneracy factor g_2 does not affect too much the total evaporative rates F_n. The branching ratios Br_1 is modified. However, in order to be consistent with the binding energies determined by Bréchignac *et al.*, we used the expression (A6) for g_2.

APPENDIX B

The total evaporative rate is given by

$$F_n = \frac{\int_0^\infty q_n(E,t_1)[1-\exp(-k_n(E)t_2)]dE}{\int_0^\infty q_n(E,t_1)dE} \tag{B1}$$

and the branching ratio for the loss of a monomer by

$$Br_1 = \frac{\int_0^\infty \frac{k_{n,1}(E)}{k_{n,1}(E)+k_{n,2}(E)} \{q_n(E,t_1)[1-\exp(-k_n(E)t_2)]\}dE}{\int_0^\infty q_n(E,t_1)dE}, \tag{B2}$$

where $q_n(E,t_1)$ is the probability that $Li_nH_m^+$ contains at t_1 an internal energy E. This probability is obtained by resolving the following equations:

$$\frac{dLi_nH_m^+}{dt} = k_{n+i,i}(E+D^+_{n+i,i})Li_{n+i}H_m^+ - k_n(E)Li_nH_m^+ \quad (i=1,2)$$

$$\frac{dLi_{n+i}H_m^+}{dt} = -k_{n+i,i}(E+D^+_{n+i,i})Li_{n+i}H_m^+ \quad (i=1,2), \tag{B3}$$

$$q_n(E,t_1) = A\left\{\frac{k_{n+1,1}(E+D^+_{n+1,1})}{k_{n+1,1}(E+D^+_{n+1,1})-k_n(E)} \times[\exp(-k_n(E)t_1)-\exp(-k_{n+1,1} \times(E+D^+_{n+1,1})t_1)] + \frac{k_{n+2,2}(E+D^+_{n+2,2})}{k_{n+2,2}(E+D^+_{n+2,2})-k_n(E)} \times[\exp(-k_n(E)t_1)-\exp(-k_{n+2,2} \times(E+D^+_{n+2,2})t_1)]\right\}, \tag{B4}$$

where $k_{n+2,2}(E+D^+_{n+2,2})$ and $k_{n+1,1}(E+D^+_{n+1,1})$ are the partial rates of dissociation of $Li_{n+2}H_m^+$ and $Li_{n+1}H_m^+$ parent ions, respectively, for the two different channels. A is a normalization factor. The above expressions have been established without taking into account two steps for the monomer evaporation. In the studied size range $(n+m<25)$, two successive evaporations are negligible and these simplified expressions are equivalent to those obtained in taking account a two steps evaporation process.

[1] T. Bergmann, H. Limberger, and T. P. Martin, Phys. Rev. Lett. **60**, 1767 (1988); H. G. Linberger and T. P. Martin, J. Chem. Phys. **90**, 2979 (1989).
[2] C. Bréchignac, Ph. Cahuzac, F. Carlier, M. de Frutos, J. Leygnier, and J. Ph. Roux, J. Chem. Phys. **99**, 6848 (1993).
[3] V. Boutou, M. A. Lebeault, A. R. Allouche, C. Bordas, and J. Chevaleyre, Z. Phys. D (to be published).
[4] C. Bréchignac, Ph. Cahuzac, F. Carlier, and J. Ph. Roux, Z. Phys. D **28**, 67 (1993).
[5] G. Rajagopal, R. N. Barnett, and U. Landmann, Phys. Rev. Lett. **67**, 727 (1991).
[6] P. Xia and L. A. Bloomfield, Phys. Rev. Lett. **72**, 2577 (1994).
[7] Ph. Poncharal, J.-M. L'Hermite, and P. Labastie, Chem. Phys. Lett. **253**, 463 (1996).
[8] A. Böttcher, R. Grobecker, R. Imbeck, A. Morgante, and G. Erti, J. Chem. Phys. **95**, 3756 (1991).
[9] R. Pflaum, K. Sattler, and E. Recknagel, Chem. Phys. Lett. **138**, 8 (1987).
[10] E. C. Honea, M. L. Homer, P. Labastie, and R. L. Whetten, Phys. Rev. Lett. **63**, 394 (1989); E. C. Honea, M. L. Homer, and R. L. Whetten, Phys. Rev. B **47**, 7480 (1993).
[11] Ph. Dugourd, R. R. Hudgins, and M. F. Jarrold, Chem. Phys. Lett. **267**, 186 (1997).
[12] P. Xia and L. A. Bloomfield, Phys. Rev. Lett. **70**, 1779 (1993).
[13] R. Antoine, Ph. Dugourd, D. Rayane, and M. Broyer, J. Chem. Phys. **104**, 110 (1996).
[14] B. Vezin, Ph. Dugourd, C. Bordas, D. Rayane, M. Broyer, V. Bonacic-Koutecky, J. Pittner, C. Fuchs, J. Gaus, and J. Koutecky, J. Chem. Phys. **102**, 2727 (1995).
[15] B. Vezin, Ph. Dugourd, D. Rayane, P. Labastie, J. Chevaleyre, and M. Broyer, Chem. Phys. Lett. **206**, 521 (1993).
[16] B. Vezin, Ph. Dugourd, D. Rayane, and M. Broyer, Surf. Rev. Lett. **3**, 171 (1996).
[17] V. Bonacic-Koutecky, J. Gaus, M. F. Guest, L. Cespiva, and J. Koutecky, Chem. Phys. Lett. **206**, 528 (1993).
[18] V. Bonacic-Koutecky, J. Pittner, and J. Koutecky, Chem. Phys. **210**, 313 (1996).
[19] C. Bréchignac, Ph. Cahuzac, J. Leygnier, and A. Sarfati, Phys. Rev. Lett. **70**, 2036 (1993).
[20] C. Bréchignac, H. Busch, Ph. Cahuzac, and J. Leygnier, J. Chem. Phys. **101**, 6992 (1994).
[21] L. S. Kassel, J. Phys. Chem. **32**, 225 (1928); **32**, 1065 (1928).
[22] C. E. Klots, J. Chem. Phys. **83**, 5854 (1985); Z. Phys. D **5**, 83 (1987); J. Phys. Chem. **92**, 5864 (1988).
[23] Ph. Dugourd, D. Rayane, R. Antoine, and M. Broyer, Chem. Phys. **218**, 163 (1997).
[24] R. Antoine, D. Rayane, Ph. Dugourd, B. Vezin, B. Tribollet, and M. Broyer, Surf. Rev. Lett. **3**, 545 (1996).
[25] K. P. Huber and G. Hertzberg, *Spectra of Diatomic Molecules* (Van Nostrand, New York, 1959).
[26] J. E. Mayer and M. G. Mayer, *Statistical Mechanisms* (Wiley, New York, 1940), Appendix VII.
[27] W. Forst, *Theory of Unimolecular Reactions* (Academic, New York, 1973).
[28] J. Leygnier, Ph.D. thesis, Orsay University, 1989.
[29] R. Poteau and F. Spiegelmann, J. Chem. Phys. **98**, 6540 (1993).